Proceedings Paper:
Monoranu, M. orcid.org/0000-0003-4759-0223, Ghadbeigi, H., Patrick, J. et al. (2 more authors) (2021) Chip formation mechanism during orthogonal cutting of rubber microparticles and silica nanoparticles modified epoxy of polymers. In: Medini, K. and Wuest, T., (eds.) Procedia CIRP. 9th CIRP Global Web Conference – Sustainable, resilient, and agile manufacturing and service operations : Lessons from COVID-19, 26-28 Oct 2021, Online conference. Elsevier B.V. , pp. 176-181.

https://doi.org/10.1016/j.procir.2021.10.028

Available online at www.sciencedirect.com

ScienceDirect

Procedia CIRP 103 (2021) 176–181

www.elsevier.com/locate/procedia

9th CIRP Global Web Conference – Sustainable, resilient, and agile manufacturing and service operations: Lessons from COVID-19

Chip formation mechanism during orthogonal cutting of rubber microparticles and silica nanoparticles modified epoxy polymers

Marius Monoranu[a,b,*], Hassan Ghadbeigi[b], J. Patrick A. Fairclough[b], Kevin Kerrigan[c]

[a]*Industrial Doctoral Centre in Machining Science, Advanced Manufacturing Research Centre, University of Sheffield, Rotherham, S60 5TZ, UK*
[b]*Department of Mechanical Engineerering, The University of Sheffield, Sheffield, S1 3JD, UK*
[c]*Advanced Manufacturing Research Centre, The University of Sheffield, Rotherham S60 5TZ, UK*

* Corresponding author. Tel.: +44-745-501-4034; *E-mail address:* m.monoranu@sheffield.ac.uk

Abstract

The addition of well-dispersed nanoparticles can significantly increase the mechanical properties and toughness of epoxy polymers. In this study, an epoxy resin was modified by addition of silica nanoparticles, (CTBN) rubber microparticles and a combination of both. An in-situ orthogonal cutting rig combined with high magnification and high-speed imaging system was used to determine the effects on the chip formation mechanism and machining induced damage to the material. This study indicates that chip formation in silica-modified epoxy is governed by a fracture process with large cracks both at the machined surface level and subsurface within the chip formation zone. The presence of rubber enables larger plastic deformation within the epoxy-modified polymer as the toughening mechanism of the rubber deflects the generated cracks within the primary deformation zone. The magnitude of machining induced damage was found to be lower for rubber microparticles and was correlated with a rubber toughening mechanism observed during cutting. The higher magnitude of machining induced damage of silica-modified epoxy was linked to the material's poor resistance to crack initiation and growth. These findings of the effect of rubber microparticles and silica nanoparticles on chip formation process will give engineers a greater ability to create a trade-off between filler properties vs material properties vs machining induced damage during Design for Manufacturing (DFM) stages of a product design.

Keywords: orthogonal cutting, chip formation, nanosilica and rubber modified epoxy, machining induced damage, digital image correlation

1. Introduction

Epoxy polymers are well known for their high mechanical properties, chemical and temperature resistance, adhesion to various substrates, and a low cost compared to their competitors. Therefore, they are used in a wide range of applications such as adhesive and coatings, and they act as structural matrix in high-performance polymer composites. However, due to their high cross-linked density, epoxy polymers have a poor resistance to crack initiation and growth. The addition of a second phase, which consists of well-dispersed particles, can significantly increase the toughness and mechanical properties of the epoxy polymer matrix [1], [2]. The development of composite-toughening technologies, which started in the 1980s, led to a point where epoxy composites are employed in primary load-carrying aircraft structures [3]. Toughening mechanisms are well documented in the literature for a wide range of industrially available nanoparticles and

10.1016/j.procir.2021.10.028

microparticles, especially silica and rubber, mixed in a wide range of epoxy blends [4]–[8]. However, little attention has been paid to individual effect of fillers on the machining behavior of nanoparticle-modified epoxy polymers.

In manufacturing of epoxy-based composite materials, machining operations are often required to achieve tight geometric tolerances, create difficult-to-mold features or ensure edge-of-part mechanical performance. The complex nature of the interaction between cutting tool and fibre/ matrix and the difference in mechanical properties of fibre and epoxy-based polymer during cutting can result in severe machining induced damage, including poor surface finish, matrix burn, pitting and fibre/ matrix delamination. The ultimate effect of such defects is a potential reduction in mechanical performance leading to catastrophic failure events [9]. Even though cutting and tool parameters are controlled to minimize machining induced damage, an in-depth assessment of the relation between material removal mechanism – material properties – machining induced damage is required.

Several previous polymer-specific studies have covered material removal mechanism and chip formation analysis in orthogonal machining of different polymers. Kobayashi and Saito [10] performed cutting experiments on three different polymers: polytetrafluoroethylene (PTFE), polymethylmethacrylate (PMMA) and polystyrene (PS). It was concluded that the cutting mechanism varied across the material used and that chip formation is influenced by the type of workpiece, cutting conditions and tool geometry. Further work from Saito [11] exposed the fracture mechanism occurring in cutting the above mentioned materials. In another study of ductile polymer machining [12], it was discovered that chip-workpiece separation occurs due to fracture in the deformation zone. However, the above-mentioned studies are based on thermoplastic examples, which have a different polymer chain structure compared to thermosets. The mechanical response of thermosets and thermoplastic during machining is different i.e. thermosets exhibit brittle behavior with very little strain to failure, while thermoplastics are generally ductile [13]. Because of these differences, the chip formation process and the machined surface quality is dependent on polymer type and machining parameters. Moreover, the response to heat generated during machining is different for the two types of polymers and is dependent on the glass transition temperature (T_g). Excessive heating leads to burning in the machined surface for thermoset polymers [14] and gumming for thermoplastic polymers. Wang et al. [15] analyzed the orthogonal cutting mechanism of two epoxy polymers cured with different crosslink densities. Experimental evidence provided support that fracture is a dominant mechanism in the chip formation process. Another relevant study [16] analyzed the machinability of silica and rubber modified epoxies. The incorporation of different types of filler changed the tensile and fracture behavior and hence the cutting force behavior of the epoxy blends. Moreover, the addition of particulate fillers affected the measured surface roughness of the machined samples. The authors concluded that cutting of these epoxy polymers belongs to a class of fracture problems. Despite this general conclusion, little effort has been made to study the material removal mechanism in relation to bulk polymer and filler material and mechanical properties and ensuing machining induced damage.

The present work investigates the cutting behavior of bulk and modified epoxy polymers under orthogonal cutting conditions. The effect of different types of fillers was assessed in relation to cutting force behavior, chip formation process and machining induced damage. The findings of this work can be further used towards damage-free machining, while improving the mechanical properties of epoxy-based materials by the addition of particulate fillers in a controlled manner.

2. Experimental method

2.1. Materials and processing

In this paper, the epoxy-modified polymers were based upon a single-component hot-cured epoxy formulation. The base epoxy resin was a low viscosity DGEBA (Diglycidyl ether of bis-phenol A) with an epoxide equivalent weight (EEW) of 167 g/eq (LY1564, Huntsman, UK). The silica (SiO_2) nanoparticles were supplied at a concentration of 40 wt% in a DGEBA epoxy resin (EEW of 295 g/eq, Nanopox F400, Evonik, Germany). The reactive liquid carboxyl-terminated butadiene-acrylonitrile (CTBN) rubber was obtained as a CTBN-epoxy adduct with a rubber concentration of 40 wt% in a DGEBA epoxy resin (EEW of 330 g/eq, Albipox 1000, Evonik, Germany). The curing agent was a cycloaliphatic polyamine (Aradur 2954, Huntsman, UK).

The DGEBA epoxy resin was mixed with the epoxy containing silica and/or rubber particles to give the required concentration of nanoparticles. The resulted blends were thoroughly mixed for 1 h at 400 RPM using a ‘resin mixer’ and degassed in a vacuum oven at 60 °C. The EEW of the blends were calculated and stoichiometric amounts of curing agent was added, mixed and degassed. The blends were then poured into a pre-heated steel release-coated mold and cured at 80 °C for 1 h, followed by a 2 h post-cure at 160 °C. Six epoxy formulations were used: (i) the unmodified DGEBA epoxy, the control, named D, (ii) the epoxy with silica nanoparticles in 10 and 20 % wt., termed Si10 and Si20, (iii) the epoxy with rubber microparticles in 10 and 20 % wt., termed R10 and R20, (iv) a hybrid epoxy containing silica nanoparticles in a 10% wt. and rubber microparticles in 10 % wt., resulting in a polymer with a total of 20% wt. of reinforcement particles, termed SR. These particular concentrations were used as it was previously found in the literature [4]–[8], [17] that the resulted epoxy blends provide an efficient improvement of tensile, compression and toughness properties.

2.2. Mechanical property testing

Uniaxial tensile tests were conducted in accordance with ASTM D-638 [18]. Tensile dog-bone samples were machined from the cured panels and were tested at a displacement rate of 5 mm/min. The displacement from the gauge length was measured using the integrated laser extensometer of the tensile machine (Tinius Olsen H5K-S). The tensile Young’s Modulus, E, yield stress, σ_y, and % strain at failure, ε_f were recorded. At

least 5 tests were conducted for each case and the average results was reported.

Compact tension (CT) samples were used to conduct fracture toughness tests in accordance with ASTM-5045 [19]. Meso-scale CT samples were machined to size according to ISO-13586 [20]. Sharp cracks were initiated in the specimens by tapping a fresh single-edged razor-blade into the notch using a toolmakers clamp[21]. Plane-strain initiation fracture energy, G_c, and fracture toughness, K_c, were determined from an average of 5 tests. The fracture energy was calculated using the energy method and cross checked using the alternative method listed in [19].

2.3. Thermal mechanical analysis

A Perkin Elmer Pyris Diamond thermomechanical analyzer (TMA) was used to record the glass transition temperature (T_g) of the epoxy blends. Rectangle shaped samples of 3 x 3.5 x 12.5 ± 0.1 mm were used. At the start of the test, the temperature was equilibrated at 25 °C. Specimens were then heated to 200 °C at 10 °C/min, while a constant force of 200 mN was applied. Following the analysis method outlined in ISO 11359-3: 2019 [22], the T_g was found as midpoint of the transition range using the first derivative of the dimension change versus measured temperature.

2.4. Orthogonal cutting tests

The chip formation process was analyzed in orthogonal cutting conditions using a specially designed rig attached to a Tinius Olsen 25ST benchtop tester. Further details about the cutting rig working principles and dimensions are available in the literature [23]. The enclosed setup of rig allows the observation of the cutting process under 2D plane strain conditions. The cutting process was recorded using a 2D High Speed Digital Image Correlation system (LaVision, GmbH) paired with a Navitar 12x Zoom Lens system. The cutting force was measured using a Kistler 9257B dynamometer at an acquisition rate of 10 kHz. To get the necessary data for further in-depth analysis of the chip formation process, the force and imaging signal were synchronized at a rate of 10 kHz. The DIC correlation was done relative to the first image, and a subset size of 29 x 29 pixels and a step size of 9 pixels were used. The pixel size was 0.001 mm, which resulted in an image resolution of 700 x 900 pixels.

Polymer samples were abrasive water jet machined to the required size of 25 x 25 x 3 mm ± 0.1 mm. The side of the samples were further polished using P400 grit paper to remove any machining induced damage. A DIC speckle pattern was applied using a fine coat of white paint and speckle pattern was created by spraying copier toner powder using a dust atomizer (Goodson, USA). 7 cutting tests for each sample were performed at a cutting speed of 1000 mm/min. Three depths of cut were used: 30, 50 and 100 µm. The depth of cut was measured using the digital micrometer attached at the side of the rig and further checked on the calibrated imagining system. High-speed steel cutting inserts with a rake angle α=10°, clearance angle γ=10° and edge radius r=10 ± 1.32 µm were used, while the cutting tools were replaced regularly to ensure the cutting performance was not affected by the tool wear. The tool geometry was accurately measured using a focus variation microscope, Alicona Infinite Focus SL.

2.5. Fractographic studies

A TM3030Plus tabletop SEM microscope was used to analyze the machined surface morphology in order to assess the role of the particulate fillers in the cutting process. Samples were gold coated prior to the SEM microscopy to facilitate the conductivity of the polymers.

3. Results and discussion

3.1. Glass transition properties

A glass transition temperature, T_g, of 153 °C was measured by TMA for the unmodified epoxy polymer as shown in Table 1. The addition of either silica nanoparticles or rubber microparticles showed no significant effect on the T_g measurement which has values of 151 ± 2 °C. Similar results are reported in the literature [4][17][7][24], where T_g was measured by differential scanning calorimetry (DSC) or dynamic mechanical thermal analysis (DMTA) showed no significant change when silica or rubber fillers were added to the base epoxy polymer.

Table 1. Glass transition temperature (T_g), Young's modulus (E) , Tensile strain at failure (ε), fracture toughness (K_C) and fracture energy for the epoxy polymer blends (G_C)

Name	T_g (°C) (TMA)	E (GPa)	Strain at failure (ε_f) (%)	K_C (MPa $m^{1/2}$)	G_C (J/m^2)
D	153	1.92	5.32	0.81	314
		± 0.1	± 0.44	± 0.04	± 19.2
R10	154	1.62	7.14	1.15	796
		± 0.09	± 0.16	± 0.05	± 17.87
R20	152	1.29	9.15	1.34	1429
		± 0.13	± 0.74	± 0.05	± 31.19
Si10	150	2.08	4.69	0.91	414
		± 0.12	± 0.34	± 0.03	± 10.11
Si20	151	2.35	2.97	1.05	478
		± 0.21	± 0.36	± 0.04	± 12.7
SR	149	1.73	5.43	1.21	841
		± 0.09	± 0.64	± 0.02	± 16.23

3.2. Mechanical properties

A tensile modulus of 1.92 GPa was measured for the unmodified epoxy polymer. The modulus was found to increase with nanosilica content as shown in Table 1. The data presented has a maximum variance of 7%. An increase of 8% and 22% was measured for Si10 and Si20 polymer compared to the base DGEBA epoxy. On the other hand, the presence of rubber microparticles decreases the modulus from 1.92 to 1.62 GPa for R10 polymer, and 1.29 GPa for R20. The addition of

10 % wt. of silica to the 'hybrid' epoxy blend restored the modulus to 1.73GPa. The strain at failure increased for rubber-modified epoxies and decreased for epoxies containing silica nanoparticles. This is typical for rubber toughening mechanism where the debonding of rubber microparticles reduces the strain at the crack tip and allows the epoxy to deform plastically via a void-growth mechanism [17]. A fracture energy, G_c of 314 J/m^2 was measured for the unmodified epoxy polymer as shown in Table 1. The fracture energy increased further with the addition of particle fillers. A maximum G_c of 478 J/m^2 was measured for the Si20 and 1429 J/m^2 for R20 polymer. The higher fracture energy of rubber modified epoxy was expected and it is related to the individual toughening mechanism of rubber microparticles [17]. Similar increasing trend was found for the fracture toughness, K_c. The fracture energy of the 'hybrid' epoxy, SR, increased to 841 J/m^2. This value is higher than R10 and S10, which emphasizes that both rubber and silica toughening mechanisms were present, as previously being experimentally evidenced in the literature [17] using high-resolution SEM imaging.

3.3. Cutting force evolution

The average cutting force of the epoxy polymers at a cutting depth of 30 µm is shown in Figure 1 where error bars represent the standard deviation between the tested samples. A gradual increase in cutting force is noticed for rubber modified epoxies with respect to the unmodified polymer. Statistical analysis of the results (T-tests) shows that there is a significant difference in cutting force between rubber and unmodified epoxy (p value < 0.05), while such a trend was not observed for silica and bulk epoxy. DGEBA and Si20 samples had an unstable cutting force with predominant 'stick-slip' force traces as shown in Figure 2. Furthermore, Si20 showed larger force fluctuations compared with the other samples. By contrast, R20 exhibited a steady-state behavior.

As it is shown in Figure 2, higher cutting forces were measured for the rubber-modified epoxy compared to silica and 'hybrid' polymer. This can be correlated to the fact that more energy is required to produce the fracture phenomena in rubber epoxy, as reported in Table 1. The toughening mechanism of the rubber particles initiate as the material fractures at the crack tip, which involves the cavitation of rubber particles, which generates the plastic deformation of the polymer epoxy. Hence, more energy is needed to plastically deform the material, therefore higher cutting forces measured for the rubber-modified epoxy. However, these findings contradict the results of Wang et al. [16] where the authors used DGEBA epoxy modified with 10 % wt. silica nanoparticles and rubber (CTBN) microparticles in orthogonal cutting tests with depth of cuts varying from 30 to 120 µm, a cutting speed of 180 mm/min. The cutting inserts had a rake angle (α), varying from 10° to 30° with a tip radius of <5 µm. The results indicated that cutting forces are higher for silica than rubber epoxy and no relationship was found between epoxy blends cutting force behaviour and their fracture properties. Moreover, the authors attributed the higher cutting force to the higher tensile properties of silica modified material, which could potentially led to difficulties in the chip formation process due to

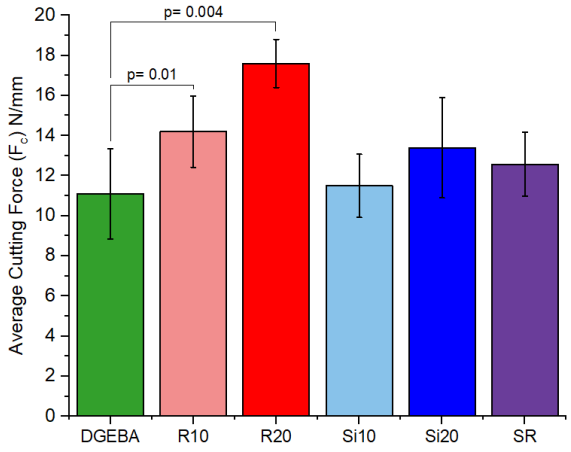

Figure 1 – Average Specific Cutting Force (F_c) for the epoxy blends at a cutting depth of 30 µm

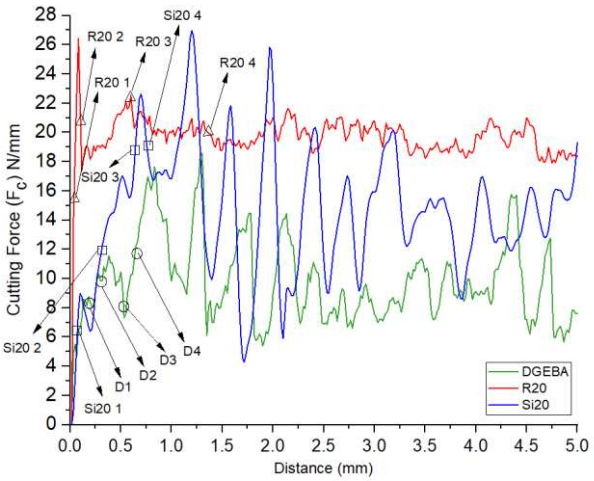

Figure 2 – Cutting force (F_c) graph for DGEBA, R20 and Si20 epoxy at a cutting depth of 30 µm

incorporation of rigid silica nanoparticles. This aspect will be clarified in Section 3.4.

3.4. Chip formation analysis and strain map evolution in relation to cutting forces and machining induced damage

Cutting frames correlated with the locations on the cutting force graph for a 30 µm depth of cut are shown in Figure 3. At the early stages of the chip formation process, the material piles-up on the rake face of the tool (Figure 3 – D1, Si20 1, R20 1). The amount of piled-up material is equal to the volume of material displaced by the tool since no crack is yet formed at the tip of the tool. An initial peak in the cutting force is found at this stage for the R20 sample, while DGEBA and Si20 samples experienced a much lower initial force. This is explained by the larger strain magnitude measured for the R20 sample (Figure 4 – c)), which undergoes plastic deformation at the tool tip within the chip formation zone. As the tool advances into the material, microcracks are generated ahead of the cutting tool (Figure 3 – D2, Si20 2). The strain fields generated for DGEBA and silica samples (Figure 4 – a) D and b) Si20) are not uniform and are pointing the possible crack initiation point. The propagation of the microcracks is facilitated by the

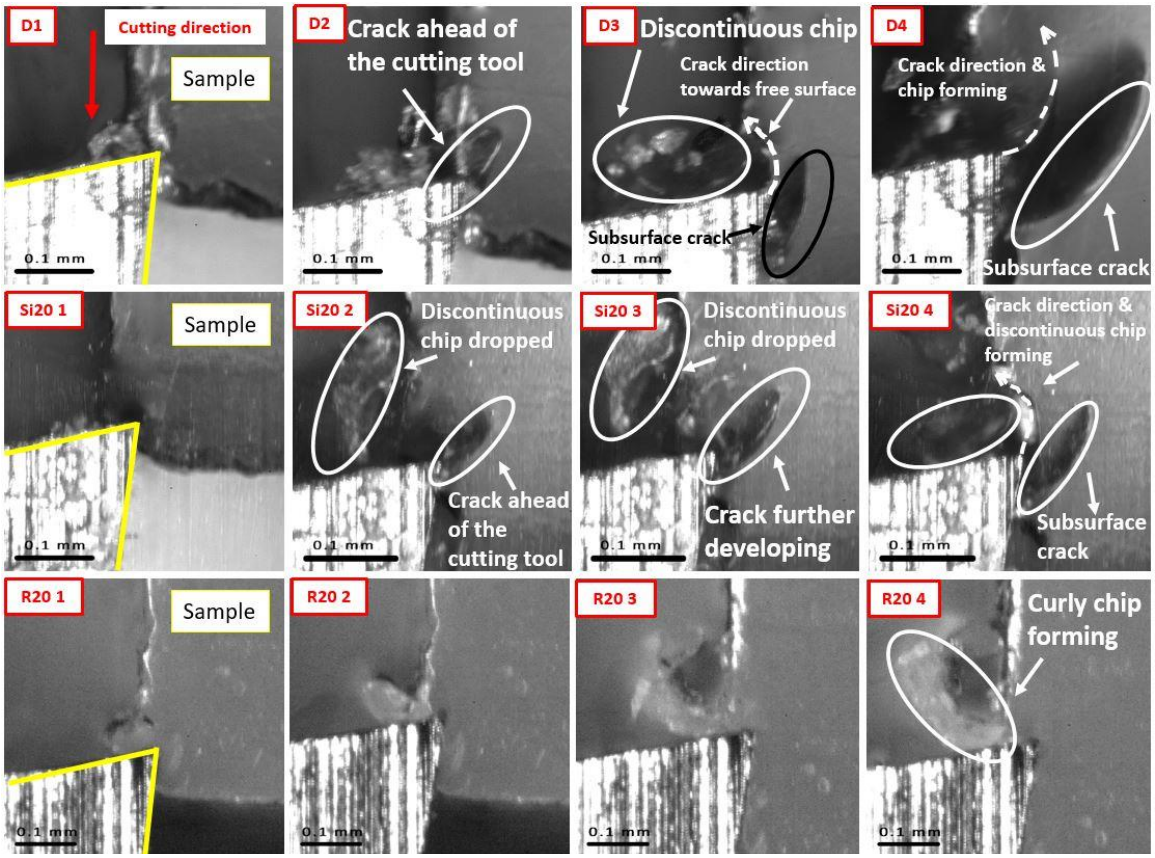

Figure 3 – Cutting frames for Cutting Force Graph shown in Figure 2 with circles showing the frame locations for D, rectangles for Si20 and triangles for R20

gradual increase of the resultant cutting force which changes from indentation (Figure 3 – D1) to complete engagement. As the friction force between the rake face and material starts gaining importance, the resultant force starts pointing towards the undeformed region of the material [25]. Additionally, the fast propagation of those cracks is associated with the low fracture toughness and strain to failure of DGEBA and silica modified epoxy. The progressively growth of the micro cracks towards the free cut surface ahead of the cutting tool (Figure 3 – D3, D4, Si20 4) generated a chip (Figure 3 – D3, Si20 2, Si20 3). However, the chip-workpiece separation stability cannot be maintained and discontinuous chips are generated, which are linked with cutting force oscillations. The oscillation starts from zero where there is no contact between the cutting tool and material. The cutting force increases gradually as a microcrack is developed in front of the cutting tool (Figure 3 – Si20 2 and Si20 3 correlated with the cutting force graph shown in Figure 2). A discontinuous chip is formed when brittle fracture occurs in front of the cutting tool (Figure 3 – Si20 4) and the force further drops and the stability of the chip-workpiece separation is no longer maintained. The start of the subsurface cracks are identified on the SEM micrographs of the machined surface (Figure 5 – a)). A zone with a smooth and glassy surface is pointed, which is typical for a brittle epoxy polymer [4]. Feather markings are noticed, which shows that crack forking took place. This phenomenon occurs when energy is absorbed fast in a brittle material and it was previously reported in the literature in fracture toughness results of silica modified polymers [4]. Similar micrographs were identified for DGEBA and Si10 samples.

Rubber modified samples formed a curly chip (Figure 3 – R20 4). The chip-workpiece separation at the tool tip is stable and is correlated with the steady state zone of the cutting forge graph. SEM micrographs of the machined surfaces (Figure 5 – b)) showed the evidence of the cavitation process enabling the subsequent toughening mechanism of plastic void growth to take place. This results in an increase plastic zone ahead of the crack tip within the polymer and the energy is dissipated creating the toughening effect. Furthermore, crack propagation ahead of the tool tip towards the undeformed material is constrained, limiting the machining induced damage. The plastic zone area is also highlighted by the uniform strain distribution shown in Figure 4 – c). It is worth mentioning that Si10 samples experienced a brittle chipping behavior, while R10 and 'hybrid' SR formed a curly chip similar to R20 samples.

At larger depth of cuts, 50 and 100 μm, the chip-workpiece separation behaved in a brittle fashion for DGEBA and silica epoxies. This phenomenon was explained previously by Atkins

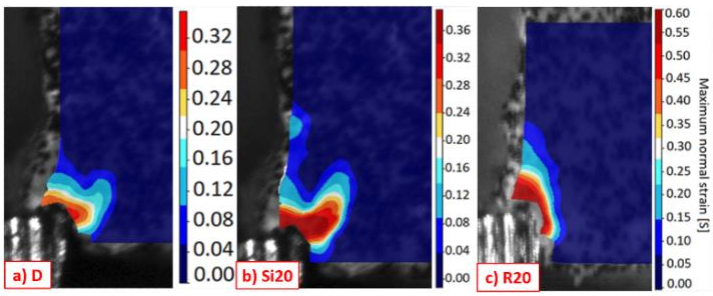

Figure 4 - Maximum normal strain [S] at the initial tool entry of the cutting tool inside the material for a) D b) Si20 c) R20

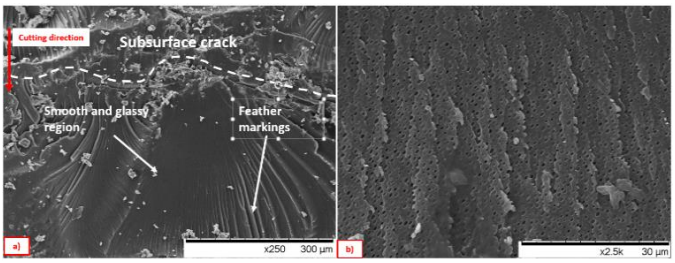

Figure 5 – SEM micrographs of the machined surfaces for a) Si20 b) R20

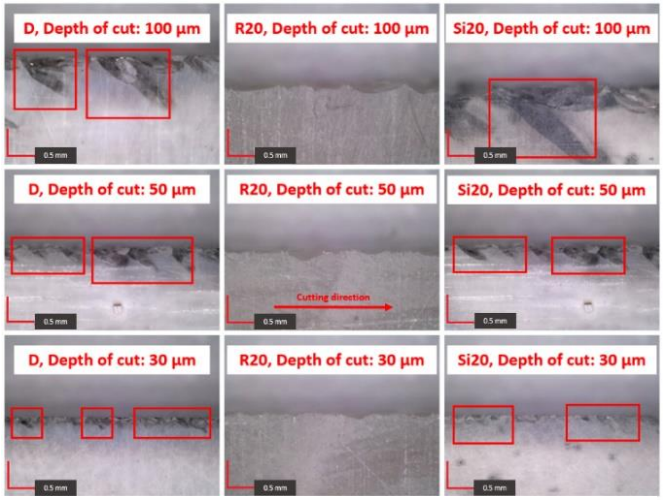

Figure 6 – Optical images of the side of DGEBA, R20 and Si20 samples machined at a depth of cut of 30, 50 and 100 µm where red rectangles show the subsurface cracks

[26] using cube-square scaling principles and successfully applied in orthogonal cutting of polymers by [15]. The cube-square scaling principle states that the energy stored in a cracked body depends on its volume, but the energy required to separate the body depends on the area of the cracked surface. Therefore, it is expected that at larger depths of cut, the fracture will be brittle with larger cracks. Experimental evidence showed that cracks length is increasing with depth of cut (see Figure 6). The material is removed by a brittle process of 'knocking lumps out' [27]. This phenomenon resulted in highly unstable cutting forces, which cannot be used for comparison with the other epoxy blends. Similar behavior was found in the literature in orthogonal cutting of other epoxy polymers [15], [27]. On the other hand, rubber modified epoxy samples produced a continuous chip at larger depth of cuts. This is correlated with the previously explained void growth mechanism and the large strain to failure of the rubber material. Additionally, the cracks are also constrained due to the plastic deformation of the material within the chip formation zone.

Conclusions

The effect of silica nanoparticles and rubber microparticles on chip formation mechanism and machining induced damage under orthogonal cutting conditions was investigated. Rubber modified epoxies experienced the highest cutting force, while no significant difference was found between DGEBA vs silica vs 'hybrid' epoxy. Experimental evidence showed that chip formation mechanism is governed by a series of intermittent fractures occurring in front of the cutting tool. Chip formation in bulk and silica-modified polymer produced discontinuous chips with large cracks at the machined surface level and subsurface within the chip formation zone. This was linked with the low fracture toughness measured for the brittle epoxies. On the other hand, rubber modified material produced a continuous curly chip due to large plastic deformation of material as the toughening mechanism of rubber microparticles was present. At the same time, the microcracks were constrained within the chip formation zone. The 'hybrid' epoxy experienced similar chip formation process as rubber samples, while the mechanical properties were close to the bulk epoxy. Future studies should focus in finding the optimal concentration of silica and rubber to provide a trade-off between machining forces, material properties and machining induced damage.

Acknowledgements

The authors would like to acknowledge the EPSRC Industrial Doctorate Centre in Machining Science (EP/L016257/1) for the funding of this work and to Huntsman, UK for the supply of the base epoxy resin.

References

[1] R. Bagheri, B. T. Marouf, and R. A. Pearson, "Rubber-toughened epoxies: A critical review," *Polym. Rev.*, vol. 49, no. 3, pp. 201–225, 2009, doi: 10.1080/15583720903048227.
[2] D. Carolan, A. Ivankovic, A. J. Kinloch, S. Sprenger, and A. C. Taylor, "Toughened carbon fibre-reinforced polymer composites with nanoparticle-modified epoxy matrices," *J. Mater. Sci.*, vol. 52, no. 3, pp. 1767–1788, 2017, doi: 10.1007/s10853-016-0468-5.
[3] D. R. Tenney, J. Davis John G., N. J. Johnston, R. B. Pipes, and J. F. McGuire, "Structural Framework for Flight I: NASA's Role in Development of Advanced Composite Materials for Aircraft and Space Structures," *Nasa/Cr–2019-220267*, vol. II, pp. 0–496, 2019, [Online]. Available: https://ntrs.nasa.gov/search.jsp?R=20190002562%0Ahttps://ntrs.nasa.gov/search.jsp?R=20190002561.
[4] B. B. Johnsen, A. J. Kinloch, R. D. Mohammed, A. C. Taylor, and S. Sprenger, "Toughening mechanisms of nanoparticle-modified epoxy polymers," *Polymer (Guildf).*, vol. 48, no. 2, pp. 530–541, 2007, doi: 10.1016/j.polymer.2006.11.038.
[5] Y. Huang and A. J. Kinloch, "The role of plastic void growth in the fracture of rubber-toughened epoxy polymers," *J. Mater. Sci. Lett.*, vol. 11, no. 8, pp. 484–487, 1992, doi: 10.1007/BF00731112.
[6] T. H. Hsieh, A. J. Kinloch, K. Masania, A. C. Taylor, and S. Sprenger, "The mechanisms and mechanics of the toughening of epoxy polymers modified with silica nanoparticles," *Polymer (Guildf).*, vol. 51, no. 26, pp. 6284–6294, 2010, doi: 10.1016/j.polymer.2010.10.048.
[7] H.-Y. Liu, G.-T. Wang, and Y. Zeng, "On fracture toughness of nano-particle modified epoxy," *Compos. Part B Eng.*, vol. 42, no. 8, pp. 2170–2175, Dec. 2011, doi: 10.1016/J.COMPOSITESB.2011.05.014.
[8] S. Sprenger, "Improving mechanical properties of fiber-reinforced composites based on epoxy resins containing industrial surface-modified silica nanoparticles: Review and outlook," *J. Compos. Mater.*, vol. 49, no. 1, pp. 53–63, 2015, doi: 10.1177/0021998313514260.
[9] M. Monoranu *et al.*, "A comparative study of the effects of milling and abrasive water jet cutting on flexural performance of CFRP," in *Procedia CIRP*, 2020, vol. 85, pp. 274–280, doi: 10.1016/j.procir.2019.09.036.
[10] A. KOBAYASHI and K. SAITO, "On the Cutting Mechanism of High Polymers," *J. Japan Soc. Test. Mater.*, vol. 9, no. 79, pp. 345–352, 1960, doi: 10.2472/jsms1952.9.345.
[11] K. Saito, "Fracture phenomena of high polymers in cutting," *J. Macromol. Sci. Part B*, vol. 19, no. 3, pp. 459–485, Jun. 1981, doi: 10.1080/00222348108015314.
[12] H. Wang, L. Chang, L. Ye, and J. G. Williams, "On the toughness measurement for ductile polymers by orthogonal cutting," *Eng. Fract. Mech.*, vol. 149, pp. 276–286, 2015, doi: 10.1016/j.engfracmech.2015.06.067.
[13] J. Y. Sheikh-Ahmad, *Machining of polymer composites*. Springer Verlag, 2008.
[14] S. Ashworth *et al.*, "Varying CFRP workpiece temperature during slotting: Effects on surface metrics, cutting forces and chip geometry," *Procedia CIRP*, vol. 85, pp. 36–41, 2020, doi: 10.1016/j.procir.2019.09.021.
[15] H. Wang, L. Chang, Y. W. Mai, L. Ye, and J. G. Williams, "An experimental study of orthogonal cutting mechanisms for epoxies with two different crosslink densities," *Int. J. Mach. Tools Manuf.*, vol. 124, pp. 117–125, 2018, doi: 10.1016/j.ijmachtools.2017.10.003.
[16] H. Wang, L. Chang, J. G. Williams, L. Ye, and Y. W. Mai, "On the machinability and surface finish of cutting nanoparticle and elastomer modified epoxy," *Mater. Des.*, vol. 109, pp. 580–589, 2016, doi: 10.1016/j.matdes.2016.07.112.
[17] T. H. Hsieh, A. J. Kinloch, K. Masania, J. Sohn Lee, A. C. Taylor, and S. Sprenger, "The toughness of epoxy polymers and fibre composites modified with rubber microparticles and silica nanoparticles," *J. Mater. Sci.*, vol. 45, no. 5, pp. 1193–1210, 2010, doi: 10.1007/s10853-009-4064-9.
[18] "ASTM D638-14, Standard Test Method for Tensile Properties of Plastics," West Conshohocken, PA, 2004. doi: 10.1520/D0638-14.1.
[19] "ASTM D5045-14, Standard Test Methods for Plane-Strain Fracture Toughness and Strain Energy Release Rate of Plastic Materials," West Conshohocken, PA, 2014. doi: 10.1520/D5045-14.
[20] "British Standards Institution, BS ISO 13586:2000, Plastics, Determination of fracture toughness (GIc and KIc): Linear elastic fracture mechanics (LEFM) approach," 2000.
[21] A. Jones, "An experimental investigation of the fracture behaviour of particulate toughened epoxies," University of Sheffield, 2013.
[22] "BS ISO 11359-3 : Plastics - Thermomechanical analysis (TMA)," 2019.
[23] Y. Guo, W. D. Compton, and S. Chandrasekar, "In situ analysis of flow dynamics and deformation fields in cutting and sliding of metals," *Proc. R. Soc. A Math. Phys. Eng. Sci.*, vol. 471, 2015.
[24] Y. L. Liang and R. A. Pearson, "The toughening mechanism in hybrid epoxy-silica-rubber nanocomposites (HESRNs)," *Polymer (Guildf).*, vol. 51, no. 21, pp. 4880–4890, 2010, doi: 10.1016/j.polymer.2010.08.052.
[25] P. A. R. Rosa, O. Kolednik, P. A. F. Martins, and A. G. Atkins, "The transient beginning to machining and the transition to steady-state cutting," *Int. J. Mach. Tools Manuf.*, vol. 47, no. 12–13, pp. 1904–1915, 2007, doi: 10.1016/j.ijmachtools.2007.03.005.
[26] T. Atkins, *The Science and Engineering of Cutting. The Mechanics and Processes of Seperating, Scratching and Puncturing Biomaterials, Metals and Non-Metals*. 2009.
[27] A. G. Atkins, "Slice-push, formation of grooves and the scale effect in cutting," *Interface Focus*, vol. 6, no. 3, 2016, doi: 10.1098/rsfs.2016.0019.